International Research Journal of Engineering and Technology (IRJET) e-ISSN: 2395-0056
Volume: 06 Issue: 11 | Nov 2019 www.irjet.net p-ISSN: 2395-0072

Optimization Design and CFD Thermal Analysis of the 72/48 Switched Reluctance Motor

Esmail Elhomdy[1,2], Zheng Liu[1], Goufeng Li[1]

[1]*School of Electrical Engineering, Dalian University of Technology, Dalian 116023, China*
[2]*Faculty of Engineering, Blue Nile University, Ad-Damazin 26613, Blue Nile State, Sudan;*

Abstract – *In this study, an overall optimization of the switched reluctance motor (SRM) is proposed to the design assessment of high-torque low-speed direct-drive in a mining application. A method of reducing computational time for multi-objective optimization based on surrogate model is proposed. A method of the design optimization of a 72/48 SRM based on Kriging model with 5 independents design variables (IDV) is presented. The objective function to maximize efficiency is investigated. In the process of electric motor design, it is important to predict and provide an accurate thermal model. The thermal analyses carried out by the method of the computational fluid dynamics (CFD) have led to a more precise evaluation of the temperatures in the various parts of the SRM. The optimization results have been successfully validated using the finite element analysis (FEA). The water jacket configuration with 17 channels was found to be optimal for the SRM, which may reduce the temperature of the motor. A 2D FEA simulation outcomes show that the 72/48 SRM direct-drive has better characteristics to replacement the conventional motor option in mining applications.*

Key Words: Computational Fluid Dynamics, Particle Swarm Optimization, Finite Element Analysis, Optimization, Sensitivity Analysis, Switched Reluctance Motor, Surrogate Model.

1. INTRODUCTION

Modern electrical machines are designed to operate under certain conditions and for specific purposes. Application of direct drive motor system has become an irresistible trend in the last decade as the knowledge of energy consumption optimization increased. The SRM used for Pulverizing machine in mining application is usually required to be with high-torque and low-speed [1]. The design procedure of SRM is complicated, which has a large number of variables and geometrical parameters. Further, it has numerous applied constraints have to be satisfied, the applied constraints refer to the maximum acceptable value of current density, the volume of the motor as well as weight of SRM. Additionally, SRM has high torque ripple, must be to minimize [2-5].

Surrogate models (SMs) based on the design of experiments (DoE) and stochastic evolutionary methods are two techniques employed for electric machine design optimization [6]. The Latin hypercube sampling (LHS) is a type of DoE. The LHS is a random sampling method that has the benefits of flexibility and a good space-filling property [7]. The number of experiments in the LHS is controllable. SMs has recently been used in machine design [8, 9]. Stochastic evolutionary methods (SEMs), such as genetic algorithm (GA) and particle swarm optimization (PSO) [10], are appropriate in electric machine design optimization because they can search a high dimension of the design space in a computationally efficient technique [11]. The SEMs have been combining with a finite-element analysis (FEA) in order to optimize the performance of SRMs [12, 13]. The electric machine design optimization methods combining SMs and SEMs reduced the computational cost. Thus, the SMs is recommended for the electric machine design optimization [12, 13].

Determination of thermal behavior of the machine is great importance, as well as the implementation of the suitable cooling system for machine. Reducing the temperature rise of the machine can be improving the performance and reliability of the motor [14, 15].

The investigation, optimization and CFD thermal analysis of the SRM with high-torque low speed in mining application are aims at this work. The flowchart process of Multi-objective (MO) optimization based on the SMs for the SRM is starting with 5 IDV, as shows in Figure 2. Based on the sensitivity analysis, the number of design elements is reduced. Following, to improve the accuracy of the SMs and the feasibility of DoE, Kriging models are constructed by performing LHS. The constructed optimal Kriging models consist of only significant designs variables. Then, a PSO-based MO optimization is performed based on the constructed SMs, with significantly reduced computational cost. Another significant of the thermal behavior of the SRM is presented. The results, including the generated Kriging models and the optimal designs, are compared with those obtained from the traditional design methods using the FEA solver to verify low computational cost and the high accuracy and of the proposed design optimization framework.

2. Design Specification and Optimization of 72/48 SRM

The SRMs have simple structure makes their designs less complicated. The design of the 72/48 SRM has the same

volume of the gear system employed in Pulverizing machine. Therefore, the primary design identifications of the SRM are listed in Table 1 [1].

Table -1: Design specification of the SRM

Design Variable	Definition	Design Variable	Definition
Rated Speed	105 rpm	Stator out diameter D_{so}	1000[mm]
Rated Power	75 kW	Rotor out diameter D_{ro}	798 [mm]
Average torque	7 kN·m	Stack length L_{stk}	340 [mm]
Length of airgap g	1 [mm]		

The diagram of the prototype the 72/48 SRM is presented in Figure 1. However, in order to precisely define the SRM geometric structure, there are still some independents design items to be considered, as follows. Therefore, the pole arcs β_{sp} and β_{rp} selection have some limitations [1] as follows:

$$\begin{aligned} \beta_{rp} &\geq \beta_{sp} \\ \min(\beta_{rp}, \beta_{sp}) &\geq \frac{2\pi}{qP_r} \\ \beta_{rp} + \beta_{sp} &< \frac{2\pi}{P_r} \end{aligned} \quad (1)$$

where P_r is the number of rotor poles and q is number of phases.

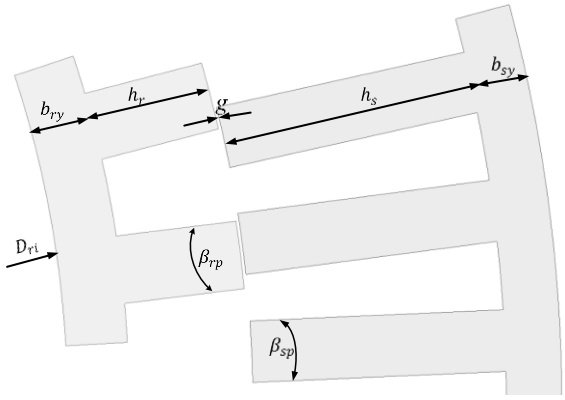

Fig -1 The construction of prototype 72/48 SRM.

The dimensions values of yoke length b_{sy} and the slot depth h_s of the stator are determined by:

$$b_{sy} = 0.5(D_{so} - D_{ro} - 2(g + h_s)) \quad (2)$$

From Table (1) the values of the D_{so}, D_{ro} and g are specified for the SRM. Thus, the equation (2) has two unknown variables b_{sy} and $h_s$and they coupled with each other. The rotor geometric dimensions consist of the inner diameter D_{ri}, yoke length b_{ry} and the slot depth h_r, which are described by:

$$D_{ri} = D_{ro} - 2(b_{ry} + h_r) \quad (3)$$

The equation (3) has three variables D_{ri}, b_{ry} and h_r, which are dependent on each other. Therefore, from equations (1), (2) and (3), there are still 5 independents design items to be investigated for the cross-section of a 72/48 SRM. As a result, the total number of separate design variables is 5, as listed in Table 2.

Table -2: independent design variables of a 72/48 SRM

Design variable	Definition
β_{sp}	Stator pole arc angle [deg]
β_{rp}	Rotor pole arc angle [deg]
D_{ri}	Rotor inner diameter[mm]
b_{sy}	Stator yoke thickness [mm]
b_{ry}	Rotor yoke thickness [mm]

The design optimization of an SRM starts for defining the optimization frame, which is comprises the design of variables, objectives, and constraints. In order to meet the design requirements and achieve the optimal performance of the SRM, the objective of the maximum efficiency is selected for the single-objective design optimization in this paper. The subjected constraints on the optimization are the average torque and torque ripple. The average torque should be met to the required output torque of the Pulverizing machine [1]. Therefore, the optimization model can be formulated as follows

$$\begin{cases} \max: f(x_i) \\ s.t \quad \{g_1(x_i), g_2(x_i)\} \\ \underline{x}_i \leq x_i \leq \overline{x}_i, i = 1,2,\dots,5 \end{cases} \quad (4)$$

where $f(x_i)$ is efficiency as objective function, and constraint functions $g_1(x_i)$ and $g_2(x_i)$ are torque and torque ripple respectively.

$$7 \leq T_{avg} \leq 7.2 \text{ kN} \cdot \text{m} \quad (5)$$

$$30 \leq T_r \leq 25 \ \% \quad (6)$$

$x_i = [\beta_{sp}, \beta_{rp}, b_{sy}, b_{ry}, D_{sh}]$ is the vector of design variables; and $\underline{x}_i$ and $\overline{x}_i$ are the lower and upper bounds of each design variable, respectively.

The aforementioned design optimization model of the SRM has a high dimension design space. In the conventional optimal design approaches, the constraints and the objective function were carried out utilizing an FEA solver for each candidate design, which makes the process

of finding the optimal solution to the SRM design problem computationally intensive. This paper is proposing using optimization based on SMs.

3. Framework for Optimization and CFD thermal of SRM

This section introduces a comprehensive frame of design optimization of the SRM, as shown in Figure 2. The determinations of SRM design specification, such as output power, speed, and torque, which is presented the first step of the proposed methodology flowchart in Figure 2. These features are defined based on Pulverizing machine in a mining application [1]. The proposed structure begins with the optimization model equation (4). Also, it is followed by 4 main parts described in the following sections. Moreover, the 3D numerical simulations of the CFD model for water jacket configurations with different numbers of channels are investigated.

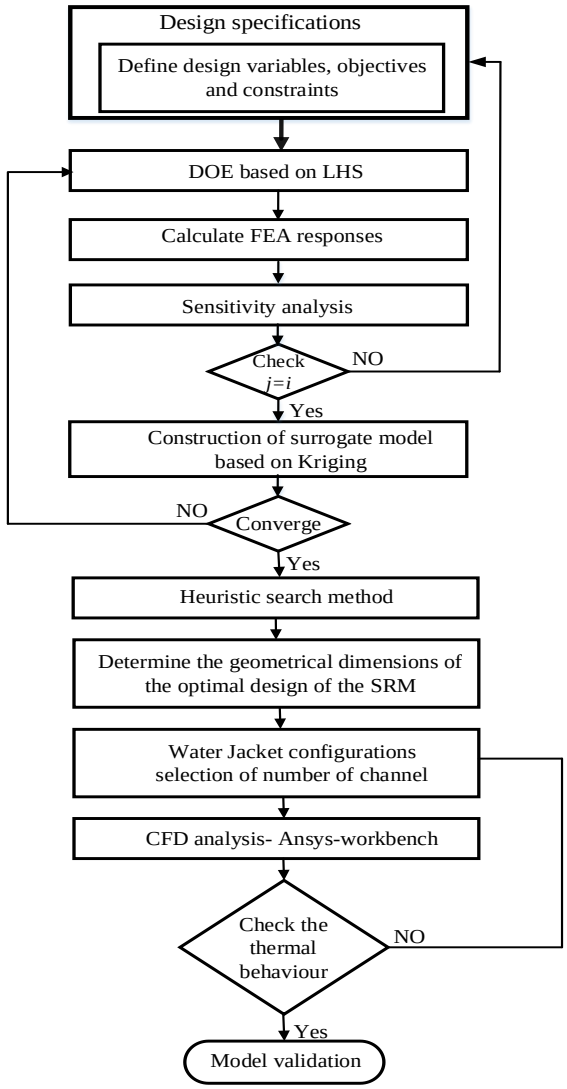

Fig -2 The Proposed overall 72/48 SRM design

3.1 Design of Experiments

DoE is aimed to collect the maximum amount of information using the minimum number of sampling points in the design spaces [12, 13, 16]. It is designed to reduce the random error and bias error in the sampling process and to make the SM more accurate. Latin hypercube sampling (LHS) [17] is a typical type of modern DoE technology extensively used in computations. Two characteristics of LHS show its advantage over the other methods. Firstly, LHS can provide a more accurate estimation of the mean value. Secondly, it is not restricted by the size of the sampling points. Therefore, it would allow the user to control the complexity and computation cost of the sampling. A simple mathematical equation for generating LHS sampling points is given by equation (7).

$$x_j^{(i)} = \frac{\pi_j^{(i)} + U_j^{(i)}}{k} \quad (7)$$

for $1 \le j \le n$ and $1 \le i \le k$, where k is the number of samples, n is the number of design variables, U is a uniform value between [0, 1], and π is an independent random permutation of the sequence of integer $0, 1, \dots, k-1$. As an improvement over the unrestricted stratified sampling method, LHS can be applied to design variables that have an abnormal probability distribution, as well as correlations among the variables [16]. Therefore, it is adopted as the preferred DoE technique in this work.

3.2 *Sensitivity Analysis for Design Space Reduction*

SA is performed first to reduce the number of design variables. SA can also provide essential insights on how each IDV affects The SRM performance. The DoE based on LHS was run in an FEA solver to calculate the machine responses, and the variance is calculated based on the simulation results. The sensitivity is measured by the sensitivity index, which is defined as follows [6 , 18]:

$$S_{x_i} = \frac{V_{x_i}(E_{x_{\sim i}}(y|x_i))}{V(y)} \quad (8)$$

The objective of this part is to analyze the effect of 5 independent design variables (IDV) on the performance of the SRM. To determine key IDV, a sensitivity study was done with 2D FEA developed in ANSYS. The model of sensitivity analysis comprises the input x_i and output y. The input is IDV x_i $[\beta_{sp}, \beta_{rp}, b_{sy}, b_{ry}, D_{ri}]$. The output y includes efficiency, ripple, and average torque. First, the sampling plan is generated for x_i using the LHS realization of 80 samples in MATLAB. Therefore, each sample point is run in the FEA (Ansys-Maxell) to obtain the output y. Then, we applied the x_i and y in equation (8). Therefore, the variance-based sensitivity indices of the three machine responses η, T_{avg} and T_r, to the 5 IDV are evaluated, and the results are shown in Figure 3. According to Figure 3, $[\beta_{sp}; \beta_{rp}]$ are significant IDV for SRM optimization. The

changes in other IDV [b_{sy}; D_{ri}; b_{ry}] have negligible effects on any of the three responses. Therefore, the number of independent design variables in the following design optimization process is reduced from 5 to 2 design variables.

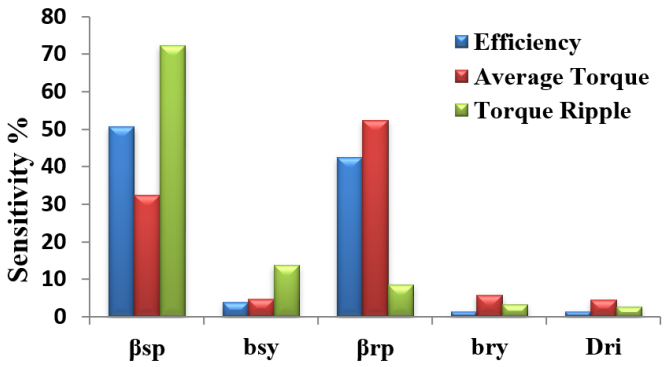

Fig -3 Sensitivity indices of efficiency, average torque, and torque ripple to the 5 IDV for the SRM.

3.3 Construction of Surrogate Models

After sensitivity analyses, the SMs are constructed by performing the DoE and FEA. The accuracy of the SMs highly depends on both the DoE and the type of SMs. Two types of SMs are generally considered: parametric and non-parametric approaches. A compromise approach called the Kriging model has become popular in recent years [8-9]. Kriging model in multi-dimensions, which is given by following the form.

$$y(x) = f(x) + z(x) \quad (9)$$

It is comprised of two parts: a polynomial f(x) and a functional departure from that polynomial Z(x). Some literature studies have been carried out to compare the precision of the SMs, and the Kriging method is considered to be reasonably accurate in predicting non-linear and real-world complex systems [19, 20]. Therefore, the Kriging model is employed in the surrogate modeling of this work.

3.4 Heuristic Search Method

Following the construction Kriging model, the optimization method should be applied to locate the local best performance. The optimization of electrical machines is a multi-variable and multi-modal problem [21-23]. At current, two major types of evolutionary optimization algorithms are commonly adopted genetic algorithm (GA) and particle swarm optimizations (PSO). PSO is a stochastic algorithm developed for optimizing continuous, nonlinear, constrained or non-constrained, non-differentiable multi-objective functions. The PSO is widely used in various fields and applied to different optimization problems [9, 23-24]. PSO has its advantages in easy implementation, having a more effective memory capability, and being more efficient in maintaining the diversity of the swarm [24-25]. In the fact that The GA presents higher computational cost and complexity than PSO, therefore PSO has been chosen for the specific optimization problem. Next, the optimization procedure is applied for the determination of numerous variables.

3.5. Thermal Analysis

Another significant is the thermal behavior of the SRM. Thus, the determination of SRM thermal behavior is essential in order to ensure high driving performance even under overload conditions and enhance the durability of insulation materials [26-28]. Thermal analysis methods of electrical machines can be divided into two basic types: analytical lumped-circuit and numerical methods. Numerical analysis is an attractive approach, as very complex geometries can be modeled, hence, the heat transfer can be accurately determined. There are two types of numerical analysis: FEA and CFD [29-30]. CFD has the advantage that it can be used to predict flow in complex regions, such as around the motor end windings. The CFD model is used to investigate the convective cooling inside the 72/48 SRM due to the circulating water, therefore computing convective heat transfer coefficient for water jacket. The 3D CFD is the best alternative for the flow process in an electrical machine. The stator core of the SRM is enfolded by the water jacket with a spiral type water channel, as shown in Figure 4. A partial sectional view of the 3D thermal model is shown as Figure 5 including stator and rotor core, shaft spoke, stator windings and housing with water channels.

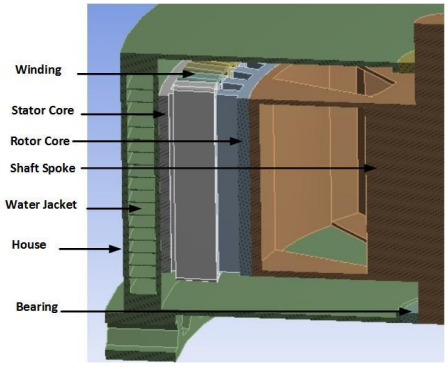

Fig -4 The sections of water jacket with a spiral type water channel with SRM.

4. Numerical test results

4.1 Optimization

The optimization plan is defined as

Maximize: η

Constraints: $7 \leq T_{avg} \leq 7.2$ kN.m

$$30 \leq T_r \leq 25$$

The range of design variables

$$2.75 \leq \beta_{sp} \leq 2.9;\ 3 \leq \beta_{rp} \leq 3.3;$$

According to the LHS plan for the SRM optimization with two IDV (β_{sp}, β_{rp}) a total of 120 sampling points have been generated, which is achieved via MATLAB software, and then each sampling point is run in the FEA (ANSYS) to obtain the results used to construct the initial surrogate model. Once the simulation results have been calculated, the efficiency and average torque contour of the SRM optimization function with two independent variables β_{sp} and β_{rp} are displayed in Figure 5.

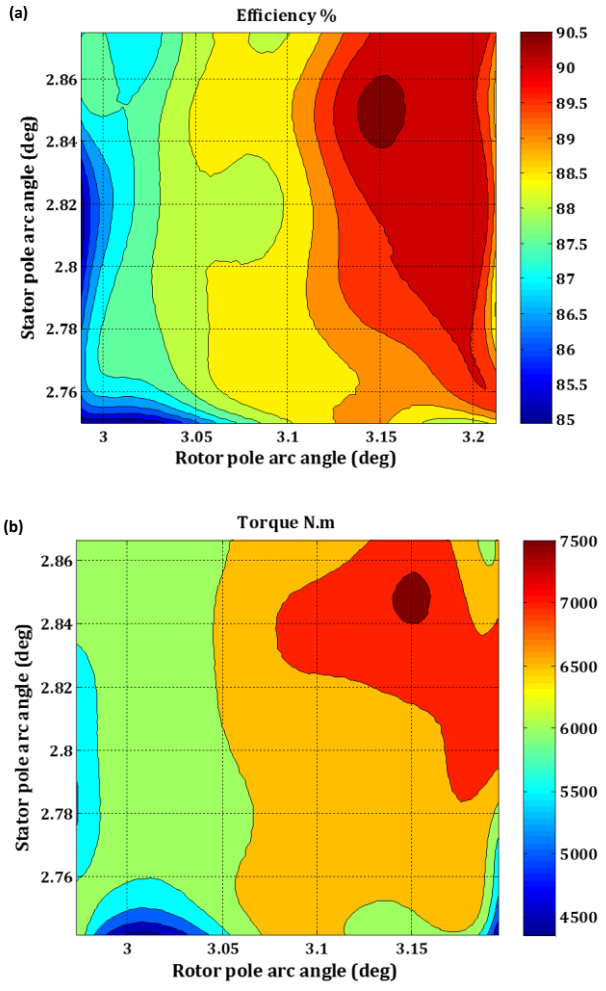

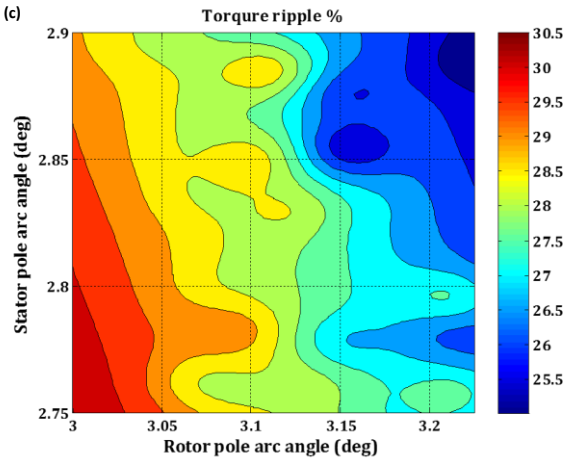

Fig -5 Preliminary surrogate results (a) Efficiency contour; (b) Average Torque contour; (c) Torque ripple contour.

Meanwhile, Three-dimensional of the efficiency and average torque versus two variables β_{sp} and β_{rp} are presented in Figure 6.

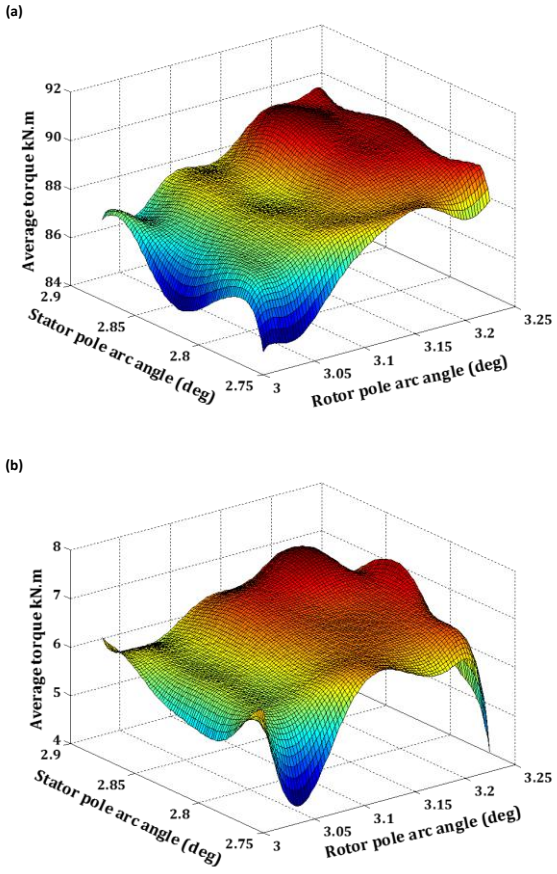

Fig -6 Three-dimensional distributions of (a) the Efficiency versus two variables β_{sp} and β_{rp} and (b) Average Torque versus two variables β_{sp} and β_{rp}.

As shown in Figures 5 and 6, the surrogate model indicates that the efficiency, average torque, and torque ripple are quite nonlinear and distributed unevenly around the entire design region. Therefore, the PSO search algorithm is adopted for optimization. Now, the surrogate model of the SRM with 2 variables has already been constructed, which can be searched for the local best point using the PSO method. The optimal final best point [β_{sp}, β_{rp},] is set at [3.15; 2.85]. Thus, the other dimensions of the 72/48 SRM are determined through equation (1) to (3). Then, the geometrical dimensions of the optimal design of the SRM are detailed in Table 3.

Table -3: the geometrical dimensions of the optimal design of the 72/48 SRM.

Parameter	Value	Parameter	Value
Number of stator poles	72	Number of stator poles	48
Rotor pole arc angle [deg]	2.851	Stator out diameter [mm]	1000
Stator pole width [mm]	19.89	Rotor pole arc angle [deg]	3.156
Stator yoke thickness [mm]	18	Rotor pole width [mm]	21.93
Stator slot depth [mm]	82	Rotor yoke thickness [mm]	20
Number of turns per pole [Turns]	15	Rotor slot depth [mm]	39
The diameter of copper wire [mm]	1.31	Rotor inner diameter [mm]	680

The values of efficiency, average torque and torque ripple at the optimal point are provided in Table 4.

Table -4: the SRM performance at optimal best point.

Parameters	Values
Efficiency [%]	90.50
Average torque [N.m]	7254.10
Torque ripple [%]	26.74

In order to verify the accuracy of the surrogate-based optimized results, FEA (ANSYS Maxwell) simulation is used to check the SRM efficiency, average torque and torque ripple with the 2 optimized design variables. To confirm the precision of the surrogate models compares to FEA, several test points (generated by LHS) are also simulated with the optimized point. The validation results are presented in Table 5.

As indicated in Table 5, the accuracy of the surrogate models (SMs) is confirmed by FEA simulation. Moreover, the electromagnetic torque of the SRM at the optimal final point was specified as functions of the time, as shown in Figure 7. Averages of the torque were obtained as 7.254 kN·m. The flux density distribution in the 72/48 SRM at rated speed 105 rpm and the optimal point can be seen in Figure 8.
The average flux densities of the stator and rotor poles are l ower than saturation value (1.7T) of (DW465-50) electrical steel laminations, which is used in the stator and rotor core.

Table-5: accuracy comparisons between FEA and surrogate model results

Item	[β_{sp}; β_{rp}] [deg]	η FEA [%]	η SMs [%]	Error [%]	T_{avg} FEA [N.m]	T_{avg} SMs [N.m]	Error [N.m]	T_{ripple} FEA [%]	T_{ripple} SMs [%]	Error [%]
Test_1	[3.00;2.76]	87.06	87.05	0.01	6097.70	6097.80	0.10	35.10	35.12	0.02
Test_2	[3.12;2.80]	89.15	89.12	0.03	6783.20	6782.90	0.30	30.48	30.45	0.03
Test_3	[3.18;2.82]	90.09	90.04	0.05	7074.58	7074.15	0.43	27.80	27.79	0.01
Test_4	[3.01;2.84]	87.12	87.13	-0.01	6109.70	6109.74	-0.04	34.99	35.02	-0.03
Test_5	[3.13;2.86]	89.55	89.57	-0.02	6907.05	6907.1	-0.05	29.16	29.17	-0.01
Test_6	[3.16;2.88]	90.15	90.10	0.05	7042.10	7041.7	0.40	27.04	27.02	0.02
Test_7	[3.18;2.89]	90.25	90.24	0.01	7107.46	7107.00	0.46	26.86	26.88	0.02
Optimized	[3.15;2.85]	90.49	90.50	-0.01	7254.10	7254.20	-0.10	26.34	26.37	-0.03

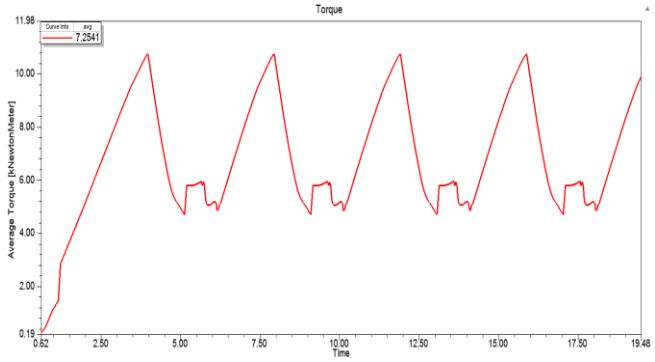

Fig -7 Averages torque of the SRM at the optimal final point

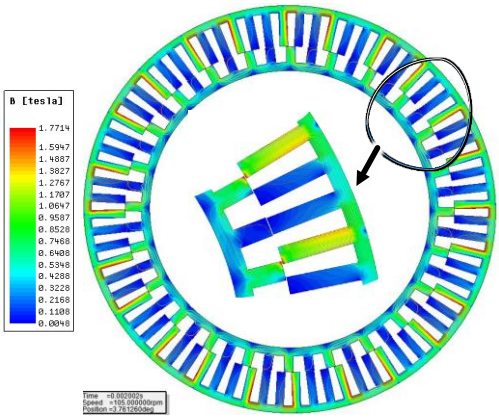

Fig -8 The distributions of the flux density of a 72/48 SRM.

4.2 CFD Simulations

The 3D numerical simulations of the CFD model for water jacket (WJ) configurations with different numbers of channels are performed, in order to selected the best number of channels. The spiral water jacket type is used, which is the coolant flows along the cylinder vertically. whereas the coolant enters cylinder from the bottom side and flow out from the head of opposite side of water jacket. The coolant used in this calculation is water at a temperature of 26 ^{o}C. For the application described in this research, the k-ε model has been used for its robustness and simplicity. The inlet and outlet boundary conditions of the coolant are defined as a mass flow inlet at a temperature of 26oC and pressure outlet respectively. The wall boundary conditions are set to heat flux boundary conditions. To estimate the temperature distribution the total losses in SRM are required inputs. The heat sources leading to the temperature rising of the motor come from all losses of the motor. These losses consist of copper loss, core loss, and mechanical loss. ANSYS finite element package was used to develop a loss model for prediction of different components of 72/48 SRM. In summary, the main losses in different portions of the 72/48 SRM are listed in Table 6.

Table -6: the losses and weight in different portions of the SRM

The portions	Values of losses [W]	The Weight [kg]
Windings	6560	199.6
Stator	1445	436.6
Rotor	650	214.6
The Total	8655	850.8

The losses of the stator, rotor with winding copper loss are mapped directly to the wall boundary conditions. Simulate and calculate the temperature rise of the 72/48 SRM under the rated load and the rated speed. The maximum temperatures in the stator winding decrease as the number of passes are increased, as the number of passes is increased beyond 17 channels for a water flow rate of 0.6 L/s, the lowering of the temperature becomes less effective. Table 7 includes a comparison between the heat transfer coefficients obtained by CFD Simulations for difference number of channels.

Table -7: a comparison of the heat transfer coefficients of different WJ configurations

WJ configuration	Heat transfer coefficients
1 channel	349
5 channels	718
9 channels	1621
17 channels	2578

For the number of channels is 17, the temperature field is uniform and symmetric in the overall of the SRM; hence, the heat dissipation of the cooling system is improved, and the result shown in Figure 9.

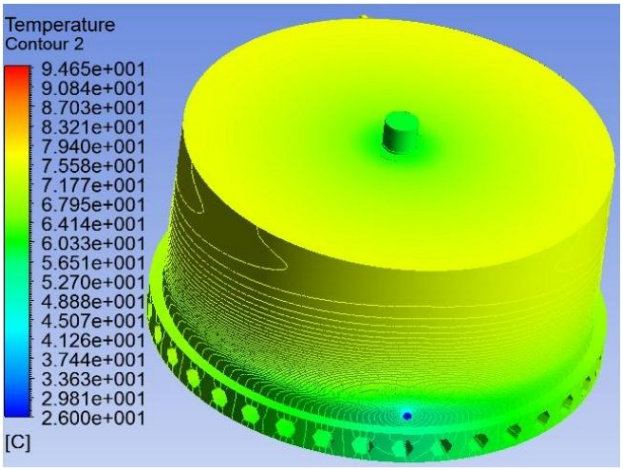

Fig -9 The 3D model's steady-state temperature profile of water jacket configurations with 17 channels.

Figure 10 shows the 3D models transient temperature profile of the SRM at flow rate 0.6 L/s. Figure 10d shows the transient temperature profile of the SRM at 55 minutes, this result similar as shown in the steady-state Figure 9.

The temperature curves for various motor parts, underrated operating, are shown in Figure 11. The temperature of the components inside the motor is stable after 55 minutes. This results in the lowering of the overall temperature field and the maximum temperature inside the motor. Therefore, we recommend used the structure of water jacket configurations, with 17 channels.

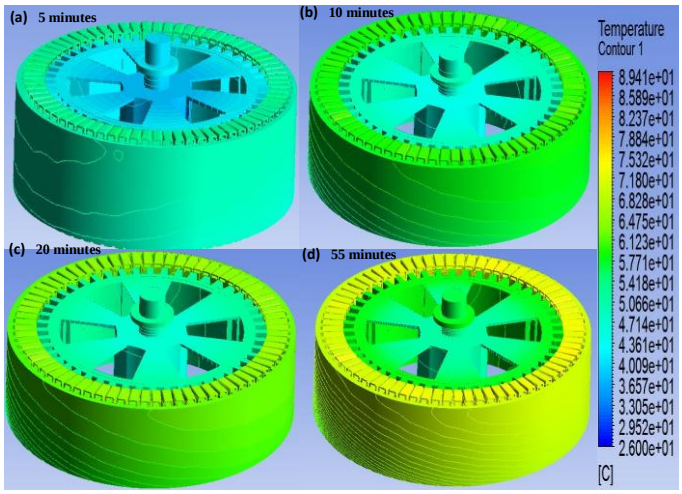

Fig -10 The 3D model's transient temperature profile of the SRM.

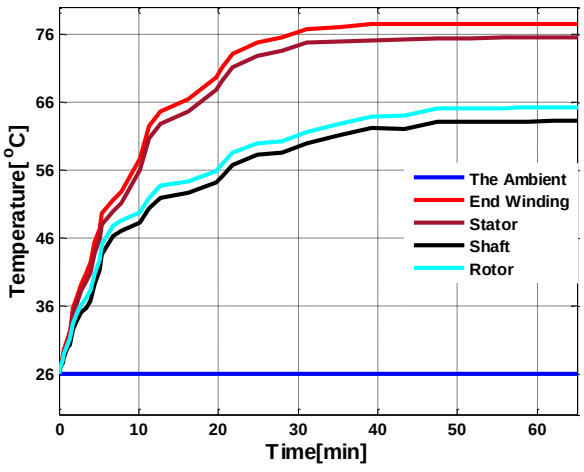

Fig -11 The CFD simulation results of the temperature rising of the various motor parts of the SRM

5. CONCLUSION

The problem of the conventional optimization computational cost has been solved by resorting to SMs. Having validated the SMs, the PSO algorithm is developed and applied to find the optimal solution. The multi-objective optimizing of the SRM design was obtained by the method of PSO based on Kriging model. The objective functions were constituted by the maximum efficiency and minimize torque ripple. Thermal Analysis of the SRM for mining applications was discussed in this paper. A 2D finite element models for the 72/48 SRM has been developed, to obtain the losses. The optimization results have been successfully validated using the finite element analysis (FEA). The cooling jacket configurations with 17 channels at flow rate of 0.6 L/s were found to be optimal for a 75 kW, 72/48 SRM. The simulation results show that the highest temperature point is 77.5°C located inside the SRM stator winding ends.

REFERENCES

[1] Elhomdy E, Li G, Liu J, et al, ''Design and Experimental Verification of a 72/48 Switched Reluctance Motor for Low-Speed Direct-Drive Mining Applications. Energies'', vol. 11, no.1, pp.192, 2018.

[2] J. H. Choi, T. H. Kim, K. B. Jang, and J. Lee, "Geometric and electrical optimization design of SR motor based on progressive quadratic response surface method," IEEE Trans. Magn., vol. 39, no. 5, pp. 3241–3243, Sep.2003.

[3] Y. K. Choi, H. S. Yoon, and C. S. Koh, "Pole-shape optimization of a switched-reluctance motor for torque ripple reduction," IEEE Trans. Magn., vol. 43, no. 4, pp. 1797–1800, Apr. 2007.

[4] F. Sahin, H. B. Ertan, and K. Leblebicioglu, "Optimum geometry for torque ripple minimization of switched reluctance motors," IEEE Trans. Energy Convers., vol. 15, no. 1, pp. 30–39, Mar. 2000.

[5] P. T. Hieu, D. H. Lee, and J. W. Ahn, "Design of 2-phase 4/2 SRM for torque ripple reduction," in Proc. Int. Conf. Elect. Mach. Syst., pp. 1–6, Oct. 2012.

[6] Ma C, Qu L, "Multi-objective Optimization of Switched Reluctance Motors Basedon Design of Experiments and Particle Swarm Optimization", IEEE Transactions on Energy Conversion, vol. 30, no. 3, pp.1-10, 2015.

[7] G. G. Wang, "Adaptive response surface method using inherited Latin hypercube design points," J. Mech. Design, vol. 125, no. 2, pp. 210–220, Jun. 2003.

[8] Yang N, Cao W , Liu Z , et al, "Novel asymmetrical rotor design for easy assembly and repair of rotor windings in synchronous generators", Magnetics Conference. IEEE, 2015.

[9] Tiejiang Yuan, Nan Yang, Wei Zhang, et al., "Improved Synchronous Machine Rotor Design for the Easy

Assembly of Excitation Coils Based on Surrogate Optimization", Energies, vol. 11, no. 5, pp.13111, 2018.

[10] J. Kennedy, "Particle swarm optimization," in Encyclopedia of Machine Learning, pp. 760-766, Springer, 2010.

[11] Santner, T.J., Williams, B.J., "Notz, W.I. The Design and Analysis of Computer Experiments", Springer: Heidelberg, Germany, 2003.

[12] Koehler, J.R., Owen, A.B., "Computer experiments", Elsevier Amsterdam, vol. 13, pp. 261–308, 1996.

[13] McKay, M.D., Beckman, R.J., Conover, W.J., "Comparison of three methods for selecting values of input variables in the analysis of output from a computer code", Technometrics, vol. 21, pp. 239–245, 1979.

[14] Karnavas YL, Chasiotis ID, Peponakis EL, "Cooling system design and thermal analysis of an electric vehicle's in-wheel PMSM", International Conference on Electrical Machines (ICEM), 4-7 2016; IEEE, Lausanne, Switzerland, pp. 1439-1445, September 2016.

[15] Jebaseeli E., Paramasivam S, "Prediction of thermal behavior of Switched Reluctance Machine using regression technique", IEEE Int. Conf. on Electrical, Computer and Communication Technologies, Coimbatore, India, pp.1–5, 2015.

[16] Giunta, A.A., Wojtkiewicz S.F., Eldred, M.S., "Overview of modern design of experiments methods for computational simulations", In Proceedings of the 41st Aerospace Sciences Meeting and Exhibit, Reno, NV, USA, pp. 6–9, January 2003.

[17] Stein, M. "Large sample properties of simulations using Latin hypercube sampling", Technometrics, Vol. 29, pp. 143–151, 1987.

[18] Wagner H M., "Global Sensitivity Analysis", Operations Research, vol. 43, no. 6, pp. 948-969, 1995.

[19] Queipo, N., Haftka, R., Shyy, W., et al, "Surrogate-based analysis and optimization". Prog. Aerosp. Sci, Vol. 41, pp. 1–28, 2005.

[20] Sasena, M.J., "Flexibility and Efficiency Enhancements for Constrained Global Design Optimization with Kriging Approximations", Ph.D. Thesis, University of Michigan, USA, 2002.

[21] X. Li and X. Yao, "Cooperatively coevolving particle swarms for large scale optimization," Evolutionary Computation, IEEE Transactions on, Vol. 16, pp. 210-224, 2012.

[22] B. Qu, P. Suganthan, J. Liang, "Differential evolution with neighborhood mutation for multimodal optimization," Evolutionary Computation, IEEE Transactions on, vol. 16, pp. 601-614, 2012.

[23] Zheng Tan, "Improved Winding Design of a Doubly Fed Induction Generator (DFIG) Wind Turbine using Surrogate Optimisation Algorithm," Ph.D. Thesis, Newcastle University, Newcastle, UK, 2015.

[24] Liu L, Liu W, Cartes D A, "Permanent Magnet Synchronous Motor Parameter Identification using Particle Swarm Optimization, vol. 4, no. 2, pp. 211-218", 2008.

[25] Ying-Nan, Qing-Ni, Hong-Fei, "Active target particle swarm optimization", Concurrency & Computation Practice & Experience, vol. 2, no. 1, pp. 29-40, 2010.

[26] Chiu H., Jang J., Yan W., et al., "Thermal performance analysis of a 30 kW switched reluctance motor", International Journal of Heat and Mass Transfer, vol. 114, pp.145–154, 2017.

[27] Wu W., Dunlop J., Collocott S., et al., "Design optimization of a switched reluctance motor by electromagnetic and thermal finite-element analysis", IEEE Trans. on Magnetics, vol. 39, no. 5, pp.3334–3336, 2003.

[28] Huang Y., Zhu Z., Guo B., et al., "Design and thermal analysis on high torque low-speed fractional-slot concentrated windings in-wheel traction motor", Electrical Machines (ICEM), XXII International Conf. IEEE, Lausanne, Switzerland , pp.1487–1492, 2016.

[29] Wang S., Zhang Y., Hu J., "Thermal Analysis of Water-Cooled Permanent Magnet Synchronous Motor for Electric Vehicles'. Applied Mechanics and Materials, vol. 610, pp.129–135, 2014.

[30] Ying X., Jinpeng G., Peng C., et al., "Coupled Fluid-Thermal Analysis for Induction Motors with Broken Bars Operating under the Rated Load", Energies, vol. no. 11, pp. 2024, 2018.

BIOGRAPHIES

Esmail Elhomdy received his B.S in Electrical Engineering and Masters in Electrical Engineering degrees from Blue Nile University and Jordan University of Science and Technology University in 2003 and 2008, respectively. He starts his PhD in Dalian University of Technology in 2014.

Zheng Liu was a Ph.D. Student with Newcastle University in 2018. Presently, he is a Postdoctoral Research at DLUT. His current research includes electric machines and drives, power electronics and Renewable Energy Technologies.

Guofeng Li was a Ph.D. Student with Dalian University of Technology (DLUT), Dalian, China, in 2000. Presently, he is a professor at DLUT. Professor Li is the dean of the School of Electrical Engineering, Dalian University of Technology (DLUT). His current research includes electric machines and drives, power electronics, Wind power generation, Electrified vehicles, Measurement techniques and Power system analysis.